Hydrodynamic Flow and Heat Transfer Characteristics of SCF

V. C. LOUKOPOULOS and G. T. KARAHALIOS
Department of Physics
University of Patras
26500 Rio, Patras
GREECE

Abstract: - We study the fundamental problem of spherical Couette flow (SCF) in the presence of heat and under the action of a gravitational field. The flow is considered as unsteady, axisymmetric and the fluid as viscous, incompressible and Newtonian. The numerical technique, which we use, is convergent and consistent and can be applied to 3D or 2D flow motions. We focus our attention to such aspect ratios $\sigma=(\bar{r}_o-\bar{r}_i)/\bar{r}_i$ for which have the presence of the important physical phenomenon of Taylor vortices formation and especially for large annular gaps, σ>0.24. Results concerning the stream function, the temperature field, the function of vorticity, the skin friction and the rate of heat transfer for large annular gap are presented. Finally, we calculate the drag acting on the inner and outer sphere and the thermal energy which is convected from the inner sphere to the fluid and from the fluid to the outer sphere.

Key-Words: - Spherical Couette flow, Taylor vortices, Drag, Thermal energy

1 Introduction

Natural convection in enclosures finds many practical applications in the many diverse fields of present engineering practice, such as the cooling of the passive cooling of advanced nuclear reactors, the double walled spherical tanks, the solar energy collector, gyroscope, geophysics fields, and the thermal storage systems [1]. It is important in these applications to realize flow field and heat transfer in enclosures considering the effect of local buoyancy.

In spite of the considerable literature on the problem going back for several decades [2], the problem has still not been fully understood and many open questions remain. The main mathematical difficulties arise from the fact that the preferred mode is usually non-axisymmetric and time dependent even at the onset of convection. In addition the relatively large number of parameters that are necessary to describe even the most simple version of the problem have complicated its investigation.

Liu et al [3] studied thermal convection in a spherical shell under an axial or a central force field both experimentally and numerically. They showed that in contrast to the axial force field for the same parameter, the flow under a central force field remains essentially axisymmetric.

Travnikov et al [4] studied the energy stability problem with respect to axisymmetric disturbances of the natural convection in the narrow gap between two spherical shells under the earth gravity. The problem was solved for different fluids with Pr=0-100 and different radius ratios n=0.9, 0.925, 0.95. They showed that there is a big difference between critical numbers for energy and linear stability theories for the small Prandtl numbers. For large Prandtl numbers this difference is very small.

Thamire and Wright [5] presented the heat transfer results, given in terms of the local and global Nusselt numbers and illustrated the effect of the flow structure on the heat transfer.

Luo and Yang [6] used linear stability analysis to determine the stability of each flow mode of spherical Taylor-Couette flow as well as the temperature distribution and heat transfer rate of each flow mode for the steady, axisymmetric, incompressible Navier-Stokes equations in a thin gap between two concentric, differentially rotating spheres. Yang and Luo also in [7] focused their study principally on the prediction of multiple steady flow patterns. The construction of bifurcation diagrams and the linear stability analysis was conducted to determine whether or not the computed steady flow solutions are stable. They used the birfucation theory to discuss the origin of the calculated flow modes.

Raghavarao and Srinivas [8] used the parametric spline function approximation to study combined convection in a rotating spherical annulus.

In a related problem Sohrab [9] discussed the flow within a droplet either located in a uniform stream or at stagnation point of axisymmetric counterflow and presented interesting results referring to the formation of Hill 's vortices within the droplet as well as to the form of these vortices as product solutions. In addition Pearlman and Sohrab [10] studied the formation of ring vortices near the equatorial plane in the case of rotating spheres.

Finally, Loukopoulos and Karahalios [11] studied the annular spherical flow numerically with a view to obtaining Taylor vortices at large aspect ratios σ such as 0.38, 0.42 and 0.48.

In this work the results of natural convection in a large spherical gap for Boussinesq fluids are presented when Taylor vortices are formed. The secondary motion, the temperature field, the function of vorticity, the skin friction and the rate of heat transfer, indicate that the flow is affected from the rotation of the boundaries, the ratio of radii and the initial conditions. Finally the form and the number of Taylor vortices are affected from the presence of temperature.

2 Problem Formulation

We consider the unsteady flow of a viscous incompressible and Newtonian fluid between two concentric and impermeable spheres. Let $\overline{r}_o$ and $\overline{r}_i$ be the radius of the outer and of the inner sphere, respectively. The subscripts i and o correspond to the inner and to the outer sphere. The overbar signifies dimensional quantities. The two shells rotate about their common vertical diameter with angular velocities $\overline{\Omega}_i$ and $\overline{\Omega}_o$ and they are maintained at constant temperatures, $\overline{T}_i$ and $\overline{T}_o$, where $\overline{T}_i > \overline{T}_o$. In addition a homogeneous gravity field acts parallel to the axis of rotation, Fig. 1. In spherical coordinates $(\overline{r},\theta,\varphi)$, let $(\overline{u}_r,\overline{u}_\theta,\overline{u}_\varphi)$ be the velocity components of the fluid.

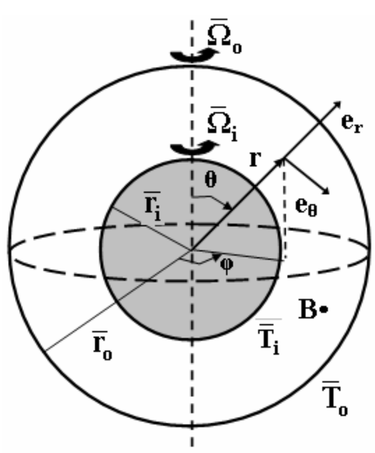

Fig. 1. Spherical annulus.

The flow is described by Navier-Stokes equations of motion

$$\frac{\partial \overline{\mathbf{u}}}{\partial \overline{t}} + \overline{\mathbf{u}} \cdot \nabla \cdot \overline{\mathbf{u}} = -\frac{1}{\overline{\rho}} \nabla \overline{p} + \overline{\nu} \nabla \cdot \overline{\mathbf{u}} + \overline{\mathbf{F}} ,$$

the continuity equation

$$\nabla \cdot \overline{\mathbf{u}} = 0 ,$$

and the energy equation

$$\frac{\partial \overline{T}}{\partial \overline{t}} + \overline{\mathbf{u}} \cdot \nabla \overline{T} = \frac{\overline{\kappa}}{\overline{\rho}\, \overline{c}_p} \nabla^2 \overline{T} ,$$

where $\overline{T}$ denotes the fluid temperature at the point $B(\overline{r},\theta,\varphi)$, $\overline{\mathbf{F}}$ is the external force per unit mass acting on the fluid, $\overline{\rho}$ is the density, $\overline{\nu}$ is the coefficient of the kinematic viscosity, $\overline{c}_p$ is the specific heat at constant pressure of the fluid, $\overline{\kappa}$ is the coefficient of thermal conductivity and

$$\nabla^{*2} = \frac{\partial^2}{\partial r^{*2}} + \frac{2}{r^*} \frac{\partial}{\partial r^*} + \frac{\cos\theta}{r^{*2} \sin\theta} \frac{\partial}{\partial \theta} + \frac{1}{r^{*2}} \frac{\partial^2}{\partial \theta^2} .$$

Since the flow is symmetric about the axis of rotation, all quantities are independent of the azimuthal angle φ.

The boundary conditions of the problem are:

Inner sphere $\overline{r} = \overline{r}_i$: $\overline{u}_r = 0$, $\overline{u}_\theta = 0$, $\overline{T} = \overline{T}_i$.

Outer sphere $\overline{r} = \overline{r}_o$: $\overline{u}_r = 0$, $\overline{u}_\theta = 0$, $\overline{T} = \overline{T}_o$.

3 Problem Solution

3.1 Numerical technique

For the solution of the problem, which is described by a coupled and non linear system of PDEs, with their appropriate boundary conditions, the stream function - vorticity formulation is used. In the numerical approach these equations are solved by dividing the region on a meridional plane $\overline{r}_i \le \overline{r} \le \overline{r}_o$, $0 \le \theta \le \pi$ into a grid of mesh points formed by lines of constant $\overline{r}$ and constant θ. The equations are approximated in terms of finite differences at each point. Next, an efficient numerical technique, constructed by Loukopoulos [12] is used in order that an algebraic system of linear equations is obtained of which the matrices of the coefficients of the unknowns are diagonally dominant. Accordingly, the corresponding equations can be solved by iterative methods (i.e. SOR) and finally a time-marching solution can be obtained. This technique can be applied to 3D or 2D flow motions and has also been used in the case of biomagnetic fluid dynamics (BFD) by Loukopoulos and Tzirtzilakis [13].

3.2 Spherical annular gap σ=0.38

Depending on the aspect ratio $\sigma=(\bar{r}_o-\bar{r}_i)/\bar{r}_i$, the Grashof number $Gr=\bar{r}_i^3\bar{\beta}\,\bar{g}(\bar{T}_i-\bar{T}_o)/\bar{\nu}$ and the Reynolds number of the flow $Re=\bar{\Omega}_c\,\bar{r}_i^2/\bar{\nu}$, spherical Couette flow exhibits certain states characterized by the formation of Taylor vortices. In the above notations $\bar{\Omega}_c$ is the characteristic angular velocity of the inner sphere, $\bar{\beta}$ is the thermal expansion coefficient and $\bar{g}$ is the acceleration of gravity. Additionally, we consider that the Prandtl number $Pr=\bar{\rho}\,\bar{c}_p\bar{\nu}/\bar{\kappa}$ is unity in all our calculations.

Our main effort is focused on the case of large gaps. In our study both sells are set into rotation from rest with different angular accelerations. Actually, for σ = 0.38 and 0.42 we start at $t=0$ with zero initial conditions at both boundaries and impose a stepwise variation in the Reynolds number and in the angular velocities according to the scheme $Re=Re_0\,n\,\Delta t$, $\Omega_i=\Omega_c\,n\,\Delta t$ and $\Omega_o=-0.3\Omega_c\,n\,\Delta t$, where n = 0,1,2,3… and Re_0 is the final value of the Reynolds number, until $t=n\,\Delta t=1$. In the above notation Δt is the dimensionless time-step. Next, for $t\geq 1$, we keep constant the Reynolds number of the flow and the angular velocity of the inner sphere and decelerate the counterrotating outer sphere to zero, with the same time-step as before. Thus $\Omega_o=0$ at $t=2$ and from then on the only varying independent parameter is time.

The most important flow and heat transfer characteristics are the local skin friction coefficient and the local rate of heat transfer coefficient. These quantities are defined by the following relations

$$C_{f_\theta}=\frac{2\bar{\tau}_\theta}{\bar{\rho}\,\bar{u}_c^{\,2}},\quad C_{f_\varphi}=\frac{2\bar{\tau}_\varphi}{\bar{\rho}\,\bar{u}_c^{\,2}}\quad Nu=\frac{\dot{\bar{q}}\bar{R}}{\bar{k}(\bar{T}_i-\bar{T}_o)}. \tag{1}$$

where $\bar{\tau}_\theta=\bar{\mu}(\partial\bar{u}_\theta/\partial\bar{r})\big|_{\bar{r}=\bar{r}_i,\bar{r}_o}$ or $\bar{\tau}_\varphi=\bar{\mu}(\partial\bar{u}_\varphi/\partial\bar{r})\big|_{\bar{r}=\bar{r}_i,\bar{r}_o}$ are the wall shear stresses and $\dot{\bar{q}}=-\bar{k}(\partial\bar{T}/\partial\bar{r})\big|_{\bar{r}=\bar{r}_i,\bar{r}_o}$ is the heat flux between the fluid and the spheres. The indices θ and φ denote the secondary and the primary flow, while $\bar{u}_c$ is a characteristic velocity and $\bar{r}_i$ a characteristic length. By the use of $\bar{u}_r=\frac{1}{\bar{r}^2\sin\theta}\frac{\partial\bar{\Psi}}{\partial\theta}$, $\bar{u}_\theta=-\frac{1}{\bar{r}\sin\theta}\frac{\partial\bar{\Psi}}{\partial\bar{r}}$, $\bar{\Psi}=\bar{r}_i^3\bar{\Omega}_c\Psi$, $\bar{\chi}=\bar{r}_i^2\bar{\Omega}_c\,\chi$, $\bar{r}=\bar{r}_i\,r$, $T=\frac{\bar{T}-\bar{T}_o}{\bar{T}_i-\bar{T}_o}$, $\tau_\theta=\frac{\bar{\tau}_\theta\bar{r}_i}{\bar{\mu}\bar{u}_c}$, $\tau_\varphi=\frac{\bar{\tau}_\varphi\bar{r}_i}{\bar{\mu}\bar{u}_c}$ (where $\bar{u}_r$ and $\bar{u}_\theta$ are the radial and meridional components of velocity respectively, $\bar{\Psi}$ is the stream function, $\bar{\chi}$ is the function of circumferential velocity and $\bar{T}$ is the function of temperature), the previous mentioned quantities can be written as

$$C_{f_\theta}=-\frac{2}{Re}\left(-\frac{1}{r^2\sin\theta}\frac{\partial\Psi}{\partial r}+\frac{1}{r\sin\theta}\frac{\partial^2\Psi}{\partial r^2}\right)\Bigg|_{r=1,1+\sigma}\quad\text{and}$$

$$\tau_\theta=-\left(-\frac{1}{r^2\sin\theta}\frac{\partial\Psi}{\partial r}+\frac{1}{r\sin\theta}\frac{\partial^2\Psi}{\partial r^2}\right)\Bigg|_{r=1,1+\sigma} \tag{2}$$

$$C_{f_\varphi}=2\left(-\frac{1}{r^2\sin\theta}\chi+\frac{1}{r\sin\theta}\frac{\partial\chi}{\partial r}\right)\Bigg|_{r=1,1+\sigma}\quad\text{and}$$

$$\tau_\varphi=Re\left(-\frac{1}{r^2\sin\theta}\chi+\frac{1}{r\sin\theta}\frac{\partial\chi}{\partial r}\right)\Bigg|_{r=1,1+\sigma}, \tag{3}$$

$Nu=-\frac{\partial T}{\partial r}\Big|_{r=1,1+\sigma}$, where Nu is the Nusselt number.

Figure 2(a) shows the 0-vortex flow mode at $Re=1050$, $Gr=3.805\times10^3$, $\sigma=0.38$ and $\Delta t=10^{-3}$. For simplicity, we depict the domain as rectangular, although it is actually curved. The solid curves designate counter-clockwise circulation, and the dashed curves clockwise circulation. In these flows, Ekman pumping causes fluid to be thrown outward centrifugally along the rotating inner sphere and pulled from the center of the stationary outer sphere, causing large-scale meridional flow whose direction is counter-clockwise in the northern hemisphere, and clockwise in the southern hemisphere. This large-scale circulation can be seen in all flows with non-zero Reynolds numbers.

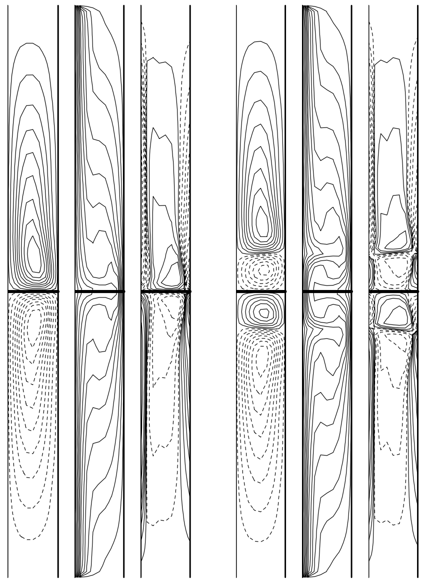

(a) (b) (c) (d) (e) (f)

Fig. 2: Different modes of flow at the same supercritical Reynolds number $Re=1050$, $Gr=3.805\times10^3$ and $\sigma=0.38$. Lines of constant streamfunction, temperature and a function of vorticity are plotted, (a, b, c) 0-vortex, (d, e, f) 1-vortex.

In Figs. 2(b) and 2(c) we show the isotherms and the distribution of the vorticity function in the meridional plane for the 0-vortex mode at $Re=1050$, $Gr=3.805\times10^3$ and $\sigma=0.38$.

In Fig. 2(d) we have plotted the streamlines distribution of the 1-vortex mode and in Fig. 2(e) we show the isotherms for the same mode for $Re=1050$, $Gr=3.805\times10^3$ and $\sigma=0.38$. The streamlines distribution of the mode shows radial inflow formed at the poles and the equator, and radial outflow formed between the vortices and large-scale cells on either side of the equator. Furthermore, isotherms twisted outward or inward at certain locations correspond to the radial outflow and inflow respectively. Finally, the lines of the vorticity function are presented in Fig. 2(f).

Figure 3(a) shows the local hemispheric Nusselt number distributions for 0-vortex mode when $Re=1050$, $Gr=3.805\times10^3$ and $\sigma=0.38$. The solid and dashed lines depict the local Nusselt numbers for the inner and the outer spheres (Nu_i, Nu_o), respectively.

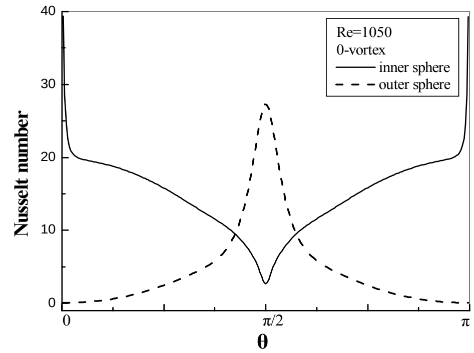

(a)

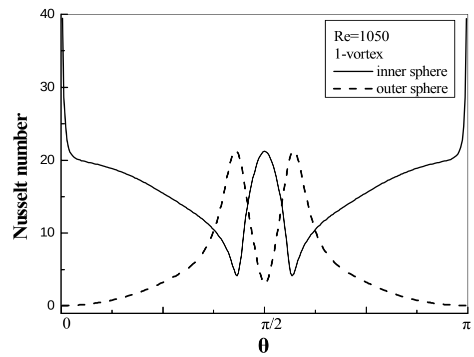

(b)

Fig. 3: (a) Local Nusselt number distribution of 0-vortex mode, (b) Local Nusselt number distribution of 1-vortex mode.

Fig. 3(b) shows the local Nusselt number distributions for 1-vortex mode when $Re=1050$, $Gr=3.805\times10^3$ and $\sigma=0.38$. Nu_i and Nu_o distribution tendencies can thus be determined by these radial inflow and outflow characteristics. At the poles and equator, Nu_i and Nu_o are locally maxima and minima, respectively. However, at the boundaries between the vortices and large-scale cells, Nu_i and Nu_o are locally minima and maxima, respectively.

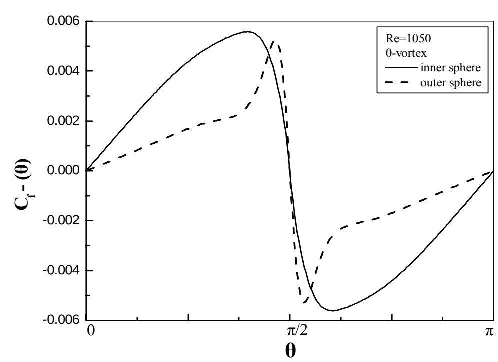

(a)

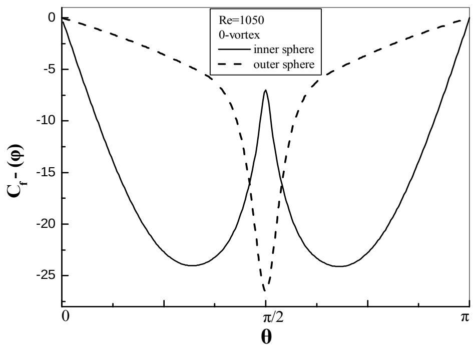

(b)

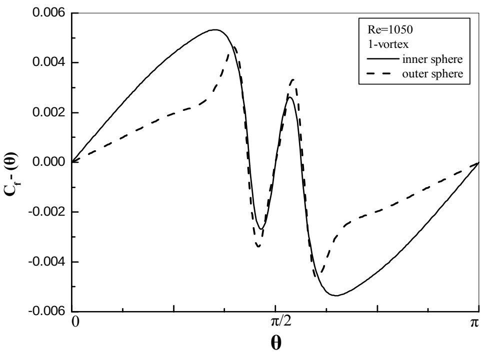

(c)

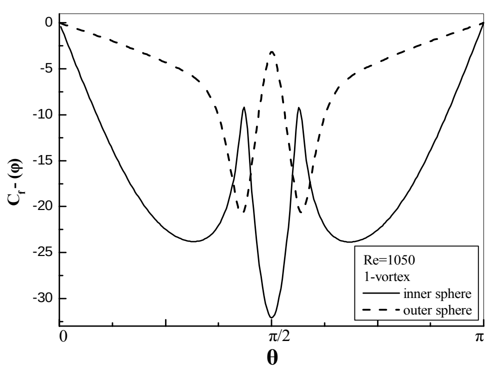

(d)

Fig. 4: Local skin friction coefficient, (a) 0-vortex (secondary flow), (b) 0-vortex (primary flow), (c) 1-vortex (secondary flow), (d) 1-vortex (primary flow).

Figure 4 presents the local skin friction coefficient, in the case of 0-vortex (secondary flow, Fig. 4(a)), 0-vortex (primary flow, 4(b)), 1-vortex (secondary flow, 4(c)) and 1-vortex (primary flow, 4(d)), respectively.

With the use of the wall shear parameter and the relations (1) to (3) it is possible to calculate the Drag D_i and D_o acting on the inner and outer sphere, respectively. So, the drag is given by the relations

$$\bar{D}_\theta\Big|_{\bar{r}=\bar{r}_i,\bar{r}_o} = \int_0^\pi \bar{\tau}_\theta\Big|_{\bar{r}=\bar{r}_i,\bar{r}_o} d\theta = -\frac{\bar{\mu}\,\bar{u}_c}{\bar{R}}\int_0^\pi \left(-\frac{1}{r^2\sin\theta}\frac{\partial\Psi}{\partial r} + \frac{1}{r\sin\theta}\frac{\partial^2\Psi}{\partial r^2} \right)\Bigg|_{r=1,1+\sigma},$$

$$\bar{D}_\varphi\Big|_{\bar{r}=\bar{r}_i,\bar{r}_o} = \int_0^\pi \bar{\tau}_\varphi\Big|_{\bar{r}=\bar{r}_i,\bar{r}_o} d\theta = 2\int_0^\pi \left(-\frac{1}{r^2\sin\theta}\chi + \frac{1}{r\sin\theta}\frac{\partial\chi}{\partial r} \right)\Bigg|_{r=1,1+\sigma}.$$

Calculation of the above mentioned integral gives that $D_\theta\big|_o / D_\theta\big|_i = 0.6383$ and $D_\varphi\big|_o / D_\varphi\big|_i = 0.3198$ for the 0-vortex flow and $D_\theta\big|_o / D_\theta\big|_i = 0.6367$ and $D_\varphi\big|_o / D_\varphi\big|_i = 0.3416$ for the case of 1-vortex flow.

From the previous results, the following conclusions can be drawn:
i) For the 0-vortex mode the drag acting on the outer sphere is 36.17% less than that of the inner for the secondary flow and 68.02% for the primary flow.
ii) For the 1-vortex mode the drag acting on the outer sphere is 36.33% less than that of the inner for the secondary flow and 65.84% for the primary flow.
iii) The foregoing calculations show that the drag ratios for the secondary and the primary flow are nearly the same for both flow modes. Actually there is a slight decrease in the secondary-flow drag ratio and a slight increase in the primary-flow drag ratio when the flow mode changes from 0-vortex mode to 1-vortex mode.

The rate of heat transfer between a sphere and the fluid, i.e. the thermal energy convected from a sphere to the fluid or reversely, per unit area and per unit time (J m^{-2} s^{-1}) is given from the Fourier law of thermal conductivity

$$\dot{\bar{q}}_{wall} = -\bar{k}\left(\frac{\partial\bar{T}}{\partial\bar{r}}\right)\Bigg|_{\bar{r}=\bar{r}_i,\bar{r}_o} = -\bar{k}\,\frac{\bar{T}_i-\bar{T}_o}{\bar{R}}\left(\frac{\partial T}{\partial r}\right)\Bigg|_{r=1,1+\sigma}.$$

From the previous relation it is possible to calculate the thermal energy Q_i and Q_o convected from the inner sphere to the fluid and from the fluid to the outer sphere, respectively. So, we have the relation

$$\overline{Q}_{i,o} = \int_0^{\pi} \dot{\overline{q}}_{wall} d\theta = -\overline{k}\frac{\overline{T}_i - \overline{T}_o}{\overline{R}} \int_0^{\pi} \left(\frac{\partial T}{\partial r} \right) \bigg|_{r=1,1+\sigma} d\theta \, .$$

Calculating of the previous mentioned integral we obtain that $Q_i/Q_o = 3.07$ in the case of 0-vortex mode and $Q_i/Q_o = 2.88$ in the case of 1-vortex mode. Consequently, the thermal energy convected from the inner sphere to the fluid is 207% bigger than that convected from the fluid to the outer sphere in the case of 0-vortex mode and 188% bigger than that convected from the fluid to the outer sphere in the case of 1-vortex mode.

4 Conclusions

We have studied the natural convection in large rotating spherical shells when Taylor vortices are present. Also, we have demonstrated that Taylor vortices are affected from the temperature field. Finally, we have computed the most important flow and heat transfer characteristics and showed that the drag acting on the outer sphere is smaller than that of the inner for the secondary and the primary flow in the case of 0-vortex mode and 1-vortex mode. Also, the thermal energy convected from the inner sphere to the fluid is bigger than that convected from the fluid to the outer sphere for both modes of the flow.

References:

[1] H.W. Wu, W.C. Tsai, and H.M. Chou, Transient Natural Convection Heat Transfer of Fluids With Variable Viscosity Between Concentric and Vertically Eccentric Spheres, *International Journal of Heat and Mass Transfer*, Vol. 47, 2004, pp. 1685-1700.

[2] M. Ardes, F.H. Busse and J. Wicht, Thermal Convection in Rotating Spherical Shells, *Physics of the Earth and Planetary Interiors*, Vol. 99, 1997, pp. 55-67.

[3] M. Liu, C. Egbers and H.J. Rath, Three-Dimensional Finite-Amplitude Thermal Convection in a Spherical Shell, *Advances in Space Research*, Vol. 16, 1995, pp. 105-108.

[4] V.V. Travnikov, H.J. Rath and C. Egbers, Stability of Natural Convection Between Spherical Shells: Energy Theory, *International Journal of Heat and Mass Transfer*, Vol. 45, 2002, pp. 4227-4235.

[5] C. Thamire and N.T. Wright, Multiple and Unsteady Solutions for Buoyancy Driven Flows in Spherical Annuli, *International Journal of Heat and Mass Transfer*, Vol. 41, 1998, pp. 4121-4138.

[6] W.J. Luo and R.J. Yang, Flow Bifurcation and Heat Transfer in a Spherical Gap, *International Journal of Heat and Mass Transfer*, Vol. 43, 1999, pp. 885-899.

[7] R.J. Yang and W.J. Luo, Flow Bifurcations in a Thin Gap Between Two Rotating Spheres, *Theoretical and Computational Fluid Dynamics*, Vol. 16, 2002, pp. 115-131.

[8] C.V. Raghavarao and S.T.P.T. Srinivas, A Numerical Study of Thermal Convection in a Rotating Spherical Annulus With Axial Gravitational Field by Using Parametric Spline Function Approximation, *International Journal of Numerical Methods for Heat & Fluid Flow*, Vol. 8, 1996, pp. 673-688.

[9] S.H. Sohrab, Modified Form of the Helmholtz Vorticity Equation and its Solution for Spherical Flow Within a Droplet in Uniform or Counterflow Streams, *IASME Transactions*, Vol. 1, 2004, pp. 634-640.

[10] H.G. Pearlman and S.H. Sohrab, Effects of Rotation on Cellular Premixed Flames Stabilized on Rotating Porous Spheres, *Combustion and Flame*, Vol. 92, 1993, pp. 469-474.

[11] V.C. Loukopoulos and G.T. Karahalios, Taylor Vortices in Annular Spherical Flow at Large Aspect Ratios, *Physics of Fluids*, Vol. 16, 2004, pp. 2708-2711.

[12] V.C. Loukopoulos, A Numerical Technique for the Solution of the Navier-Stokes Equations of Unsteady Flow, *Computer Methods in Applied Mechanics and Engineering*, Vol. 195, 2006, pp. 534-550.

[13] V.C. Loukopoulos, E.E. Tzirtzilakis, Biomagnetic Chanel Flow in Spatially Varying Magnetic Field, *International Journal of Engineering Science*, Vol. 42, 2004, pp. 571-590.